Effects of absorption on beam coupling gain in photorefractive materials (BSO) under strong modulation with an external applied electric field

I. Casar and L.F. Magaña
Instituto de Física, Universidad Nacional Autónoma de México
Apartado postal 20-364, 01000 México D.F.,Mexico
e-mail: fernando@fenix.ifisicacu.unam.mx

Recibido el 25 de febrero de 1998; aceptado el 14 de mayo de 1998

We numerically calculated the steady-state beam coupling gain for two wave mixing with absorption in BSO under strong modulation of the light intensity. First, the coupling gain coefficient was obtained. Then, the variation of the intensities of the two interfering beams along the thickness of the sample was calculated for a typical case having an applied d.c electric field of 5 Kv/cm. We compare our results with those obtained with no absorption. The effects of absorption are drastic and the gain coefficient has a limiting value, as we go deeper in the sample. This limiting value is independent of the initial value of the beam coupling coefficient at the surface of the sample and is also independent of the value of the absorption coefficient.

Keywords: Photorefractive effect, non-linear optics

Calculamos numéricamente, para el estado estacionario, el coeficiente de ganancia de acoplamiento de dos haces de luz que interfieren en un material fotorrefractivo BSO con absorción y con una alta modulación en la intensidad de luz. Primero, se calculó el coeficiente de ganancia de acoplamiento; luego, se calculó la variación, a lo largo del espesor de la muesta, de las intensidades de los dos haces que interfieren, para un caso típico y teniendo un campo eléctrico aplicado de corriente directa de 5 Kv/cm. Hacemos una comparación con resultados obtenidos cuando no hay absorción. Encontramos que los efectos de la absorción son drásticos y que el coeficiente de ganancia de acoplamiento tiene un valor límite conforme nos adentramos en la muestra. Este valor límite es independiente del valor inicial del coeficiente de acoplamiento a la entrada de la muestra y es independiente también del valor del coeficiente de absorción.

Descriptores: Efecto fotorrefractivo, óptica no lineal

PACS: 42.40.Eq; 42.70.Mp

1. Introduction

Photorefractive materials have an important technological potential [1-3] due to their capacity to store great quantities of information (10^{12} bits per cm^3, *i.e.*, around 10^3 times more than magnetic memories) and to their ability to exchange energy, by the coupling of light beams which may lead to coherent light amplification. Recording is obtained through a variation in the refractive index within the material. To optimize the recording in these materials high modulations of the light pattern must be used and the effects of absorption of energy by the material have to be taken into account. Nevertheless, due to the complexity of the phenomena the usual way to describe the photorefractive effect is with a linear approach (low modulation of the light pattern).

In this work we take a rigorous approach. We present nonlinear numerical calculations of beam coupling gain taking into account high modulations and absorption. The experimental geometry we used is shown in Fig. 1, with a sinusoidal light interference pattern: $I = I_0(1 + m\cos kx)$. The numerical method consists of two steps. The first is the numerical solution of the material equations to obtain the amplitude and the phase, ϕ, of the fundamental Fourier component of the space charge field, as functions of m. With this information

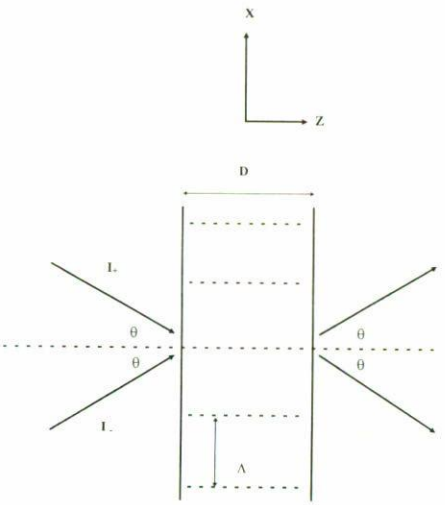

FIGURE 1. Diagram of the experimental configuration.

the gain coefficient can be immediately calculated, also as a function of m. The second part, then, is the numerical solution of the equations for the coupled beams. For this part we rewrite the beam coupling equations to consider absorption and to have differential equations for m as a function of z.

TABLE I. Values of the physical parameters for BSO used in the numerical solution of the material rate equations.

$I_0 = 5$ mW/cm^2 (Average light intensity)
$\varepsilon = 56$ (Dielectric constant)
$n = 2.53$ (Refractive index)
$r = 5.0 \text{ X } 10^{-12}$ (electroptic coefficient)
$N = 10^{25}$ m^{-3} (Donor density)
$N_A = 10^{22}$ m^{-3} (Acceptor density)
$A = 10\ \mu$m (Grating period)

The calculations were performed for BSO with usual physical parameters (see Refs. 4–6) as given in Table I, an applied electric field of 5 KV/cm, an average light intensity of $I_0 = 5$ mW/cm^2 and several possible values of the absorption coefficient, α, between 0 and 1 cm^{-1} [7]. All this was done for several values of m between 0 and 1.

2. Material rate equations

Using the band transport model, the response of the photorefractive material, that is, the carrier transport from the bright to the dark areas arise from: carrier diffusion, electric–field induced drift and the photovoltaic effect. Neglecting the photovoltaic effect and assuming electron transport, the rate equations governing the physical response of the photorefractive material are [1–4]

$$\frac{\partial N^+}{\partial t} = (sI + \beta)(N - N^+) - \gamma n N^+, \tag{1a}$$

$$\frac{\partial n}{\partial t} = \frac{\partial N^+}{\partial t} + \frac{\partial}{\partial x}\left(D\frac{\partial n}{\partial x} + \mu n E\right), \tag{1b}$$

$$\frac{\partial(\varepsilon\,\varepsilon_0\,E)}{\partial x} = e(N^+ - N_A - n), \tag{1c}$$

where the motion of the carriers is along x, N_A is the initial number of acceptors, N^+ is the concentration of acceptors at instant t and N the total concentration of traps. The electron concentration is n and their mobility μ, D is the diffusion coefficient, γ the trapping coefficient, β the thermal ionization rate, s the photoionization cross section, ε the dielectric constant and ε_0 the permitivity in free space. The total electric field is E and is given by the sum of the applied field E_a and the space charged field E_{esc}.

We solved differential Eqs. (1) following the method of lines that uses finite element collocation procedure, with time–independent secondary degree polynomials for the discretization of the spatial variable x. The details are given in Ref. 4. The solution was obtained from 10^{-10} seconds up to 4 seconds, *i.e.* until the stationary state was reached. This was done for values of m between 0 and 1.

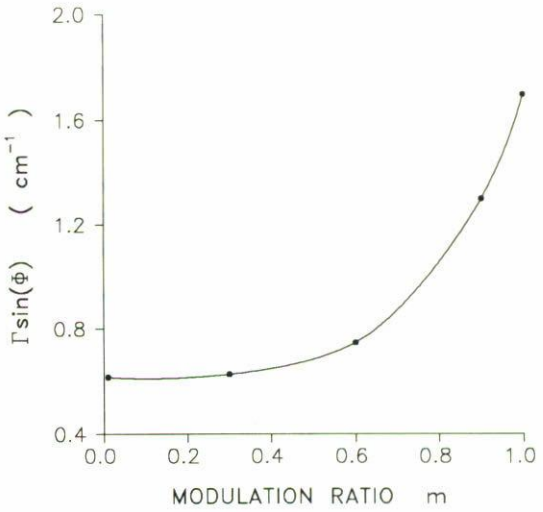

FIGURE 2. Gain coefficient as a function of m.

From the solution of the set of Eqs. (1) we obtained the space charge field, the carrier and the donor densities. Having the space charge field we obtained its fundamental Fourier component and the phase of this in order to calculate the gain coefficient, $\Gamma \sin\phi$, as a function of m, which is shown in Fig. 2.

3. Beam coupling equations

We used the coupled wave formulation described in Ref. 8. The beam coupling equations were solved numerically using the beam coupling gain, $\Gamma \sin\phi$, obtained above, which for untilted gratings, neglecting optical activity and absorption coefficient α, can be written as [8]

$$\frac{dI_+(z)}{dz} + \Gamma \sin\phi \left[\frac{I_+(z)I_-(z)}{I_0}\right] - \alpha I_+(z) = 0, \tag{2a}$$

$$\frac{dI_-(z)}{dz} - \Gamma \sin\phi \left[\frac{I_+(z)I_-(z)}{I_0}\right] - \alpha I_-(z) = 0, \tag{2b}$$

where $\Gamma = 2\pi n^3 r E_l/(m\lambda\cos\theta)$, λ is the light wave length of the beams, θ the incidence angle, r the effective electroptic coefficient, n is the refraction index and Φ is the phase of the space charge grating field with regard to the light.

On the other hand, the light modulation is changing with depth during propagation as

$$m(z) = 2\frac{[I_+(z)I_-(z)]^{1/2}}{I_0}, \tag{3a}$$

where

$$I_0 = I_{(+)}(0) + I_{(-)}(0)$$

and

$$I_+(z) + I_-(z) = I_0(z)\exp(-\alpha z). \tag{3b}$$

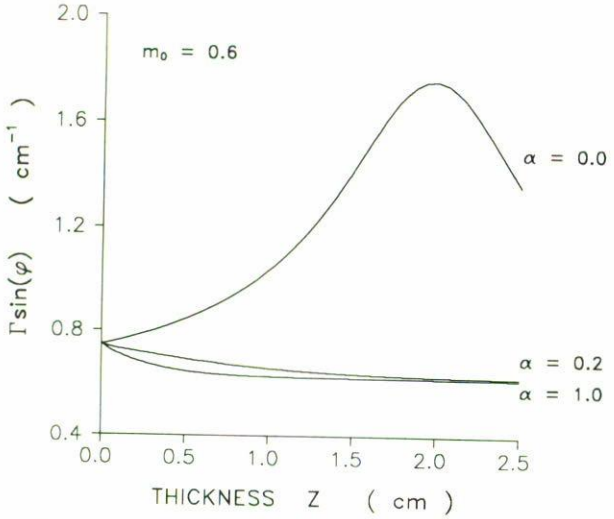

FIGURE 3. Gain coefficient as a function of z for a value of $m_0 = 0.6$ and several values of the absorption coefficient, α.

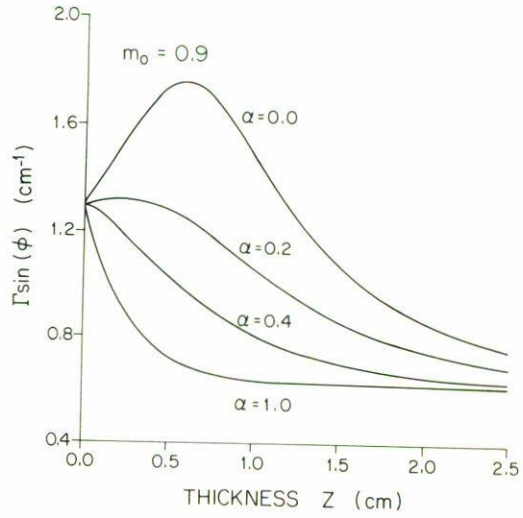

FIGURE 4. Gain coefficient as a function of z for a value of $m_0 = 0.9$ and several values of the absorption coefficient, α.

The numerical method we have used is as follows. The sample is divided into thin slabs of thickness Δz along the propagation direction z, in such a way that $m(z)$, within each slab, is practically constant (changes smaller than 0.1%). For the first slab (which starts at $z = 0$ and ends at $z = \Delta z$) the incoming light intensities are $I_+(z = 0)$ and $I_-(z = 0)$ and the modulation depth is $m(z = 0) = m_0$. With these initial conditions the amplitude $E_1[m(z = 0)]$ and the phase $\phi[m(z = 0)]$ of the recorded index grating in the first slab are taken from the first step of the analysis, *i.e.*, from numerical solution of Eqs. (1). Then, the solution of the equations within this slab for $I_+(z)$ and $I_-(z)$ are

$$I_+(z) = \left(\frac{I_0}{2}\right)\left(1 - \sqrt{1 - m_0^2}\cos\lambda z - \sin\lambda z\right) \times \exp\left(\frac{-\alpha z}{2}\right) \tag{4a}$$

$$I_-(z) = \left(\frac{I_0}{2}\right)\left(1 + \sqrt{1 - m_0^2}\cos\lambda z + \sin\lambda z\right) \times \exp\left(\frac{-\alpha z}{2}\right) \tag{4b}$$

where $\lambda = (m\Gamma\sin\phi)/2$. Next, an updated value of m for $z = \Delta z$, is obtained for $I_+(z)$ and $I_-(z)$ and this is used for the next increment in z as an initial condition. The corresponding value of $\Gamma\sin\phi$, for this new value of $m(z + \Delta z)$ is obtained by interpolation and the corresponding solutions are updated for this new slab. For the rest of the slabs we proceeded in the same fashion, until we reached the exit face of the sample.

4. Results and conclusions

The results of our numerical calculation are shown in Figs. 3 to 8. In Figs. 3 and 4 we can see a comparison of the beam

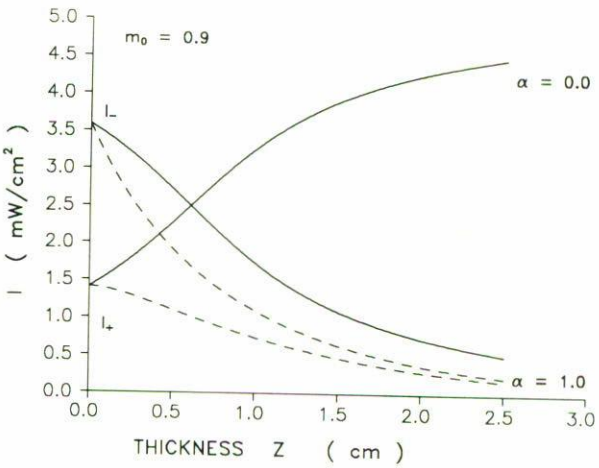

FIGURE 5. Beam coupling. Variation with z of two beams. Continuous line is with no absorption; dashed line is with an absorption coefficient of 1.0 cm^{-1}. The value of m_0 is 0.9.

coupling gain coefficient, $\Gamma\sin\phi$, with and without absorption for $m_0 = 0.6$ and $m_0 = 0.9$ respectively. The maximum of $\Gamma\sin\phi$ in both cases tends to disappear when absorption is present. This happens even for small values of the absorption coefficient, α. However, this effect diminishes with increasing m_0. Another interesting feature is that there is a limiting value of $\Gamma\sin\phi$ when z increases. This limiting value is independent of the initial value of $\Gamma\sin\phi$ at $z = 0$ and of the value of α. This must happen because $\Gamma\sin\phi$ is a function of m and from Eq. (3a), m depends on $I_+(z)$ and on $I_-(z)$ and these two tend to zero, due to absorption, as we go deeper in the material. In this fashion, for long enough z, the limiting value of $\Gamma\sin\phi$ will be the corresponding one for $m = 0$ (see

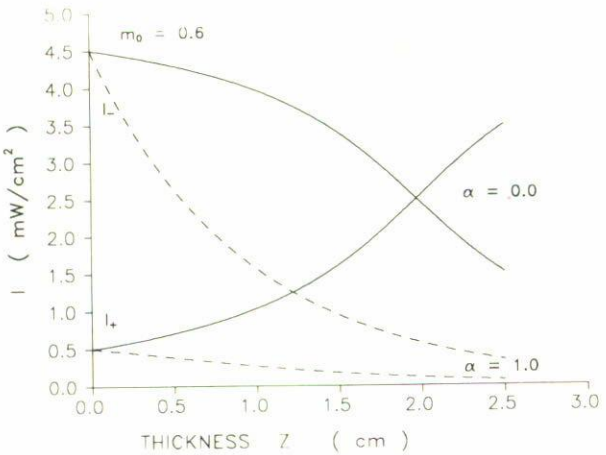

FIGURE 6. Beam coupling. Variation with z of two beams. Continuous line is with no absorption; dashed line is with an absorption coefficient of 1.0 cm^{-1}. The value of m_0 is 0.6.

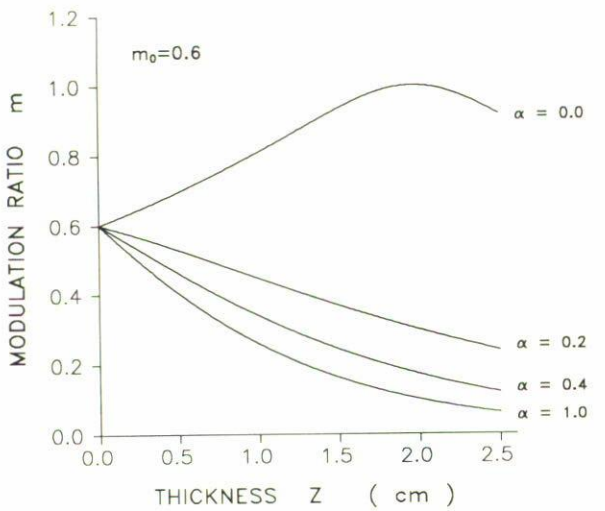

FIGURE 7. Variation of the light modulation with depth z, for a value of $m_0 = 0.6$ and several values of the absorption coefficient, α.

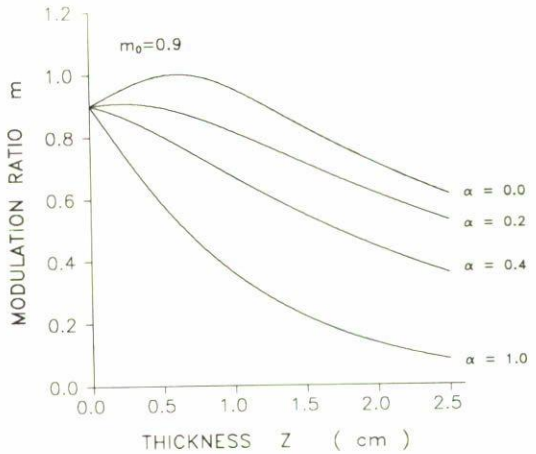

FIGURE 8. Variation of the light modulation with depth z, for a value of $m_0 = 0.9$ and several values of the absorption coefficient, α.

Fig. 2). In Fig. 5, we show the beam coupling variation of the two beams along z with and without absorption. The differences are again drastic. Even for high modulation of the light pattern the beams tend to zero rapidly, masking the energy exchange that is taking place among the beams. In Figs. 6 and 7 we show the modulation ratio m as a function of z, for $m_0 = 0.6$ and $m_0 = 0.9$ This was obtained from Eqs. (3) and (4). Again, we can see the drastic effects of absorption. The maximum for $m(z)$ disappears with absorption.

Notice that with no absorption we could choose an optimum thickness of the sample in order to obtain maximum gain. However, when absorption is present this statement is no longer valid and one should select the thinnest sample to have the optimum gain.

Acknowledgments

We want to acknowledge financial support from European Union under contract No. CT94-0039, and from DGAPA-UNAM project No. IN105697.

1. P. Günter and J. P. Huignard (editors), *Photorefractive Materials and their applications II*, (Springer Verlag, 1989).
2. Tschudi *et al.*, *IEEE J. Quantum. Electron.* **QE-221**, (1986) 1493.
3. S.I. Stepanov, *Rep. Prog. Phys.* **57** (1994) 39.
4. J.G. Murillo, L.F. Magaña, M. Carrascosa, and F. Agulló-López, *J. Appl. Phys.* **78** (1995) 5686.
5. L.B. Au and L. Solymar, *Opt. Lett.* **13** (1988) 660.
6. E. Serrano, V. Lopez, M. Carrascosa, and F. Agulló-López, *J. Opt. Soc. Am. B* **11** (1994) 670; *IEEE J. Quantum. Electron* **30** (1994) 875.
7. Kiyoshi Nakagawa, Keiji Arita, Kenji Kitamura, and Takumi Minemoto, *Proceedings of 1997 Topical Meeting on Photorefractive Materials, Effects and Devices* (PR'97), p. 419.
8. F. Agulló-López, J.M. Cabrera, and F. Agulló-Rueda, *Electrooptics: Phenomena, Materials and Applications*, (Academic. Press San Diego, 1994).